

Cross sections for inner-shell excitation of Na-like ions

Ronald J. W. Henry

Department of Physics and Astronomy, Louisiana State University, Baton Rouge, Louisiana 70803

Alfred Z. Msezane

Department of Physics, Morehouse College, Atlanta, Georgia 30314

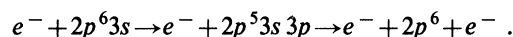
(Received 22 February 1982)

The contributions of excitation autoionization to electron-impact ionization in the Na-like Al^{2+} and Si^{3+} are calculated using a two-state close-coupling approximation. Inner-shell excitations of the type $2p^6 3s \rightarrow 2p^5 3s 3l$ ($l=0,1,2$) are included. The contributions of resonant-excitation double autoionization are estimated from a three-state close-coupling approximation with the aid of quantum-defect-theory analysis. These contributions explain the absence of the largest predicted excitation-autoionization step in the measurements of Crandall *et al.* Predictions for Mg^+ also lead to similar agreement with experiment. We conclude that the experiments of Crandall *et al.* for the total ionization cross sections for Mg^+ , Al^{2+} , and Si^{3+} by electron impact include measurements of the physical processes of direct-ionization, inner-shell excitation autoionization, and inner-shell resonant-excitation double autoionization.

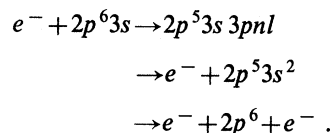
Crandall *et al.*¹ reported recently on measured absolute cross sections for electron-impact ionization of the Na-like ions Mg^+ , Al^{2+} , and Si^{3+} . The ionization data shows some anticipated excitation-autoionization structure in addition to a smooth direct ionization contribution. Such structure has been obtained previously in other systems and has been reviewed by Crandall.² Griffin *et al.*³ calculated the contributions of the excitation-autoionization process to electron-impact ionization of Mg^+ , Al^{2+} , and Si^{3+} in the distorted-wave approximation with exchange. These calculations indicated that the largest contributions were due to the $2p^6 3s \rightarrow 2p^5 3s 3p$ excitations. However, this largest predicted excitation-autoionization step is effectively absent in the measurements.¹ We show that this apparent discrepancy can be explained by an additional mechanism, the resonant-excitation—double-autoionization process, as introduced recently by LaGattuta and Hahn.⁴

We present two- and three-state close-coupling calculations for inner-shell excitation of Al^{2+} and Si^{3+} and, by extrapolation, we predict some results for Mg^+ . The eigenstates retained in the close-coupling expansion are the ground state and an excited inner-shell state of the form $2p^5 3s 3l$. For the present purposes, we are interested in the transitions $2p^6 3s \rightarrow 2p^5 3s 3l$ followed by decay by autoionization. A significant contribution to electron-impact

ionization comes from excitation of an inner-shell electron, which subsequently loses its energy by ejection of a more loosely bound electron from an outer shell. An example of this *excitation-autoionization* process is



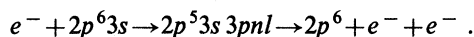
Another significant contribution to electron-impact ionization comes from the temporary capture of the incident electron with simultaneous excitation of an inner-shell electron. This resonance decays with emission of two electrons. An example of this resonant-excitation—double-autoionization (REDA⁴) process is



Another possibility is a *resonant-excitation—auto-double-ionization* (READI) process⁵ in which the incident electron is captured temporarily with simultaneous excitation of an inner-shell electron. This resonance decays with simultaneous emission of the two electrons since both electrons may be screened from the target core. An example of the READI process is

TABLE I. Energy differences and weight coefficients for eigenstates.

Ion	State	Eigenstate	C_1	C_2	C_3	ΔE (a.u.)
Al ²⁺	1	$2p^6 3s^2 S$	0.999 97	0.008 01	0.000 59	0.0
	2	$2p^5 3s^2 2P^o$	0.999 85	-0.009 59	0.013 55	2.8141
	3	$2p^5 3s^1 P^o 3p^2 D$	0.0	0.850 66	0.525 70	3.0221
	4	$2p^5 3s^1 P^o 3p^2 P$	0.0	0.832 70	0.553 73	3.0289
	5	$2p^5 3s^1 P^o 3p^2 S$	0.008 02	-0.999 46	-0.032 00	3.0737
	6	$2p^5 3s^3 P^o 3p^2 D$	0.0	0.525 70	-0.850 06	3.1700
	7	$2p^5 3s^3 P^o 3p^2 P$	0.0	0.553 73	-0.832 70	3.1840
	8	$2p^5 3s^3 P^o 3p^2 S$	-0.000 33	-0.032 01	-0.999 49	3.2113
	9	$2p^5 3p^3 P^o 3d^2 P^o$	0.003 01	-0.698 19	-0.715 90	3.4394
	10	$2p^5 3p^1 P^o 3d^2 P^o$	-0.016 34	-0.715 84	0.698 06	3.4673
Si ³⁺	1	$2p^6 3s^2 S$	0.999 98	0.006 69	0.000 36	0.0
	2	$2p^5 3s^2 2P^o$	0.999 81	-0.010 43	0.016 15	3.4779
	3	$2p^5 3s^1 P^o 3p^2 D$	0.0	9.850 89	0.525 34	3.7508
	4	$2p^5 3s^1 P^o 3p^2 P$	0.0	0.829 10	0.559 10	3.7596
	5	$2p^5 3s^1 P^o 3p^2 S$	-0.006 66	0.998 63	-0.051 83	3.8160
	6	$2p^5 3s^3 P^o 3p^2 D$	0.0	0.525 34	-0.850 89	3.9284
	7	$2p^5 3s^3 P^o 3p^2 P$	0.0	0.559 10	-0.829 10	3.9478
	8	$2p^5 3s^3 P^o 3p^2 S$	0.000 70	-0.051 83	-0.998 66	3.9990
	9	$2p^5 3p^1 P^o 3d^2 P^o$	0.002 32	-0.768 80	-0.639 47	4.3239
	10	$2p^5 3p^3 P^o 3d^2 P^o$	-0.019 10	-0.639 40	0.768 62	4.3626



This process cannot be separated from the REDA process in current experiments, although evidence for it may show up below the $2p^5 3s^2$ threshold, where REDA cannot contribute. Further, in the present calculations, we are unable to calculate a READI contribution. However, it is a physical mechanism which cannot be ignored.

The orbitals used are Slater-type orbitals obtained by Clementi and Roetti.⁶ With the CIV3 program of

Hibbert,⁷ we construct a $3d$ orbital and configuration-interaction (CI) wave functions to describe the target states. Excitation energies and configuration weights are given in Table I for Al²⁺ and Si³⁺. The dominant eigenstates are represented as follows:

$${}^2L: C_1 2p^6 3s + C_2 2p^5 3s^1 P^o 3p + C_3 2p^5 3s^3 P^o 3p ,$$

$${}^2P^o: C_1 2p^5 3s^2 + C_2 2p^5 3s^1 P^o 3d + C_3 2p^5 3s^3 P^o 3d .$$

Single-configuration states $2p^5 3s^3 P^o 3p^4 S$, 4P , and 4D ; and $2p^5 3s^3 P^o 3d^4 P^o$, ${}^4D^o$, and ${}^4F^o$ are also used in the calculations.

The coupled integrodifferential equations are solved through the use of the noniterative integral equation method of Henry *et al.*⁸ Step sizes at small radial distances are chosen to be $0.003a_0$, and exchange terms are dropped at $16.8a_0$ and $11.8a_0$ for Al²⁺ and Si³⁺, respectively, where the magnitude of the largest orbital has fallen to less than 10^{-3} .

Two-state results for the collision strengths for excitation of an inner-shell $2p$ electron are given in Table II for energies from threshold to approximately four times threshold for Al²⁺ and Si³⁺. The collision strength Ω is related to the cross section σ by

TABLE II. Collision strengths $\Omega(i,j)$ versus electron energy k^2 (Ry).

Ion	k^2	$\Omega(2p, 3s)$	$\Omega(2p, 3p)$	$\Omega(2p, 3d)$
Al ²⁺	7.35	0.040	0.46	0.10
	8.82	0.046	0.49	0.12
	14.7	0.075	0.52	0.22
	22.05	0.108	0.53	0.32
	29.4	0.133	0.54	0.40
Si ³⁺	9.4	0.043	0.46	0.12
	14.7	0.043	0.47	0.24
	22.05	0.063	0.49	0.39
	29.4	0.070	0.49	0.51
	36.75	0.096	0.50	0.60
	44.1	0.108	0.50	0.66

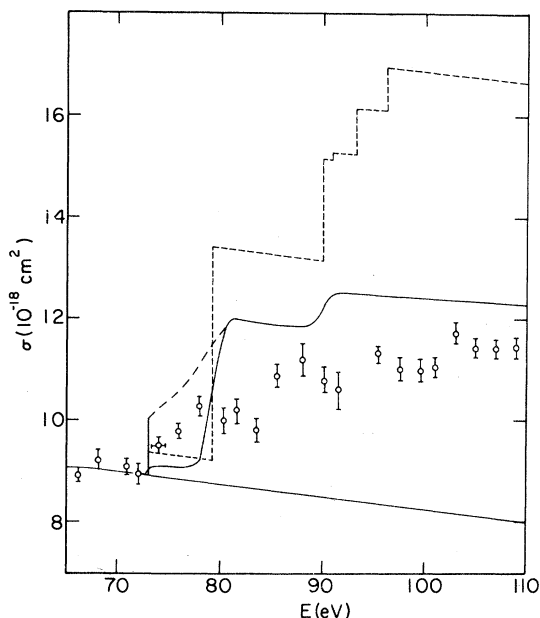


FIG. 1. Electron-impact ionization of Al^{2+} . Lower solid curve is distorted-wave calculation of direct ionization by Younger (Ref. 9), normalized to experiment at 70 eV by multiplying Younger's results by 0.65. Dashed curve is distorted-wave excitation of Griffin *et al.* (Ref. 3) added to Younger's direct-ionization results. Upper solid curve is present close-coupling excitation added to Younger's direct-ionization results. Dash-dotted curve is close-coupling excitation plus resonance effects, plus direct ionization. Open circles represent experiment of Crandall *et al.* (Ref. 1).

$$\Omega(i, j) = \omega_i k_i^2 \sigma(i \rightarrow j),$$

where ω_i (which equals 2 for this paper) is the statistical weight of the initial state i , k_i^2 (Ry) is the energy of the electron relative to state i , and the cross section σ is measured in units of πa_0^2 . The notation indicates the active electron, i.e., $2p$, $3s$, $3p$, and $3d$ are, respectively, the configurations $2p^6 3s$, $2p^5 3s^2$, $2p^5 3s 3p$, and $2p^5 3s 3d$.

The collision strengths listed exhibit the expected large-energy behavior. The dipole forbidden $\Omega(2p, 3p)$ is approximately constant whereas the others increase as $\ln k^2$. The surprise is that the monopole-dominated transitions still contribute about half of the collision strengths at four times threshold energy with even larger percentage contributions at lower energies.

Figure 1 gives electron-impact ionization cross sections for Al^{2+} in the near excitation-autoionization threshold region. The lower solid curve represents a distorted-wave calculation of direct ionization by Younger,⁹ normalized to the ex-

periment of Crandall *et al.*¹ at 70 eV by multiplying Younger's results by 0.65. A distorted-wave calculation of Griffin *et al.*³ for the excitation-autoionization process is added to Younger's scaled direct ionization results to give the dashed curve. Present results are given by the upper solid curve. Our two-state close-coupling results are added to Younger's scaled direct-ionization calculations. Further, we have convoluted our results with a 2-eV full width at half maximum (FWHM) Gaussian to simulate experimental energy spread. The dash-dotted curve represents a Gaussian average over the resonance contributions below the $3p$ threshold, as discussed below. Open circles represent measurements of Crandall *et al.*¹ Note that the distorted-wave calculations³ contain additional contributions from $2p-4l$ at energies above 90 eV, whereas the present calculations do not.

Electron-impact-ionization cross sections for Si^{3+} in the near excitation-autoionization threshold region are given in Fig. 2. The lower solid curve represents a distorted-wave calculation of direct ionization by Younger.⁹ No scaling was required to obtain reasonable agreement with experiment at energies below 100 eV. The upper solid curve and the dashed curve represent present two-state close-coupling and distorted-wave³ calculations, respectively, for the excitation-autoionization process which have been added to Younger's direct-ionization calculation. Again, we have convoluted our results with a 2-eV FWHM Gaussian to simulate experimental energy spread. The dash-dotted curve represents a Gaussian average over the resonance contribution below the $3p$ threshold, as dis-

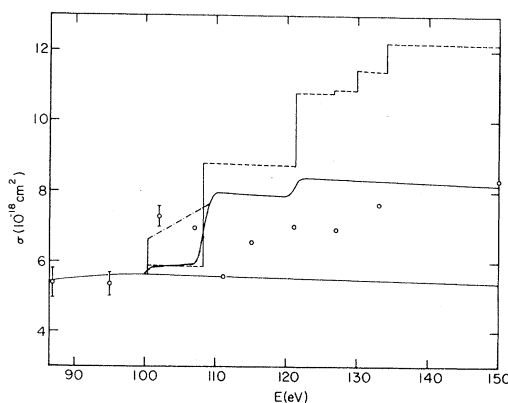


FIG. 2. Electron-impact ionization of Si^{3+} . Notation as in Fig. 1, except that the distorted-wave calculation of direct ionization by Younger (Ref. 9) is not normalized.

TABLE III. Excitation cross sections (in 10^{-18} cm 2) at threshold.

	Mg $^+$		Al $^{2+}$		Si $^{3+}$	
2p-3s	0.87 ^a	0.31 ^b	0.46 ^a	0.25 ^b	0.25 ^a	0.20 ^b
2p-3p	6.02 ^a	4.33 ^b	4.18 ^a	3.10 ^b	2.94 ^a	2.13 ^b
2p-3d	1.31 ^a	0.68 ^b	2.00 ^a	0.62 ^b	2.10 ^a	0.56 ^b

^aGriffin *et al.* (Ref. 3).

^bPresent work.

cussed below. Open circles represent measurements of Crandall *et al.*¹

We have extrapolated our results along the isoelectronic sequence to predict excitation-autoionization effects in Mg $^+$. Table III compares inner-shell excitation cross sections at threshold for Mg $^+$, Al $^{2+}$, and Si $^{3+}$ calculated in a distorted-wave approximation³ and the present two-state close-coupling approximation. Figure 3 gives electron-impact-ionization cross sections for Mg $^+$ from threshold to 70 eV. Open circles represent measurements of Crandall *et al.*¹ which have an energy spread of about 0.5-eV FWHM in the resonance region. The lower solid curve represents a distorted-wave calculation of direct ionization by Younger,⁹ normalized to experiment at 35 eV by multiplying Younger's results by 0.80. Previously,^{1,3} a scaling factor of 0.78 was used and this resulted in an unexplainable departure of the theoretical and experimental curves at 40 eV, well before the threshold energy of the $2p^5 3s^2$ configuration. This small increase in the scaling factor eliminates the apparent early onset of indirect ionization processes. The upper solid curve represents our extrapolated close-coupling results which have been added to Younger's scaled direct ionization calculations. If the scaling factor is 0.78, then an alternative explanation for the difference between the theoretical and experimental curves is that it is due to the READI process.

In Figs. 1 and 2 the distorted-wave approximation³ (DW) predicts larger cross sections for the inner-shell excitation-autoionization contribution than the present two-state close-coupling approximation (CC2). These differences have been investigated for $2p^6 3s \rightarrow 2p^5 3s 3p$. They have been found to be due to the contribution of an incident p -wave and final p -wave electron, where CC2 and DW give $0.0159\pi a_0^2$ and $0.0268\pi a_0^2$, respectively. This contribution represents, respectively, 40% and 58% of the total contribution. The differences are probably due to the treatment of the nonorthogonality terms in the DW approximation, although the authors¹⁰ estimate only a 10% effect due to the neglect of

those terms. The non- p -wave contributions are approximately the same.

In Figs. 1–3, the present two-state close-coupling calculations, when added to scaled distorted-wave direct-ionization calculations, agree fairly well in magnitude with the measurements of Crandall *et al.*¹ Recently, McGuire¹¹ found that a plane-wave Born calculation for both the direct-ionization and inner-shell excitation-autoionization processes gave agreement with measurements to better than 10% for Mg $^+$ and to within 20% for Al $^{2+}$ and Si $^{3+}$. In discussing this result, McGuire stated "This may be fortuitous, particularly near threshold."

No attempt has been made to investigate the convergence of our close-coupling approximation. The present calculation probably overestimates the excitation cross sections due to a redistribution of flux among all the accessible channels.¹² In contrast to the theoretical predictions of CC2 or DW, the experimental data for all three ions does not appear to indicate any significant increase in the total ionization cross section at the $2p^5 3s 3p$ threshold. We perform a model calculation to explain this apparent discrepancy in terms of resonant-excitation—double-autoionization effects. Insufficient detail is given by McGuire¹¹ to determine which $3l$ state is important.

In our model calculation, we consider a three-state close-coupling approximation for Al $^{2+}$ in which $2p^6 3s$, $2p^5 3s^2$, and $2p^5 3s^3 P^o 3p^2 S$ states are included. The equations are solved by the program NIEM⁸ at three energies above the excitation energy threshold for the $3p$ state $E_{th}(3p)$. Collision strengths in

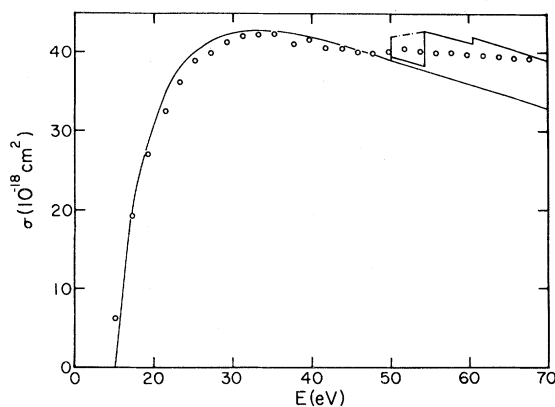


FIG. 3. Electron-impact ionization of Mg $^+$. Notation as in Fig. 1, except that the distorted-wave calculation of direct ionization by Younger (Ref. 9) is normalized to experiment at 40 eV by multiplying Younger's results by 0.80.

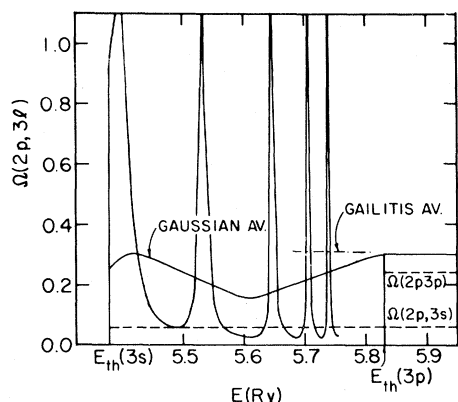


FIG. 4. Electron-impact ionization of Al^{2+} ; a model calculation which includes $2p^63s$, $2p^53s^2$, and $2p^53s^3P^o3p^2S$ states. Solid curves—three-state close coupling and convoluted with 2-eV FWHM Gaussian; dashed-curve—two-state close-coupling; dot-dash curve—Gailitis average.

the energy region between the $3s$ and $3p$ thresholds are obtained by program RANAL of Pradhan and Seaton.¹³ This program extrapolates the above threshold results and uses quantum-defect theory¹⁴ to analyze the reactance matrix elements.

Figure 4 gives the collision strength versus energy for $\Omega(2p, 3s)$, $\Omega(2p, 3p)$, and $\Omega_t(2p, 3l)$. Below the $3p$ threshold, some of the lower resonances are shown. Also, the Gailitis- and Gaussian-averaged collision strengths are given. The total collision strength is given by

$$\Omega_t(2p, 3l) = \begin{cases} \bar{\Omega}(2p, 3s), & \text{for } k^2 < E_{\text{th}}(3p) \\ \Omega(2p, 3s) + \Omega(2p, 3p), & \text{for } k^2 > E_{\text{th}}(3p) \end{cases}$$

where $\bar{\Omega}(2p, 3s)$ represents the effect of the Rydberg series of resonances below the $3p$ threshold which have been convoluted with a 2-eV FWHM Gaussian. The very large enhancement of the allowed excitation process $\Omega(2p, 3s)$ below the $3p$ threshold is due to the initial and final states being more strongly coupled to the closed $3p$ state than to each other.¹⁵ The strength of coupling may be gauged by considering collision strengths at energy levels just above the $3p$ threshold. For $\Omega^>(2p, 3s)$, $\Omega^>(2p, 3p)$, and $\Omega^>(3s, 3p)$ we obtain 0.06, 0.24, and 10.2, respectively. Through the use of a Gailitis average,¹⁶ the average collision strength below threshold can be related to the above threshold collision strengths by

$$\Omega_{\text{Gailitis}}(2p, 3s) = \Omega^>(2p, 3s) + \frac{\Omega^>(2p, 3p)\Omega^>(3p, 3s)}{\Omega^>(2p, 3p) + \Omega^>(3p, 3s)}$$

For example, $\Omega_{\text{Gailitis}}(2p, 3s)$ is 0.30, contrasted to a nonresonant collision strength of 0.06. Thus, we conclude that the contribution of resonances to the averaged collision strength is such as to remove the step function at threshold which is predicted by nonresonant approximation theories such as the two-state close-coupling, distorted-wave, or Coulomb-Born theories.¹⁷

The resonant complex which is formed by the capture of an incident electron by a $3p$ state may be labeled $2p^53s^3P^o3p^2Snl$. In our model calculation, we find that the $n=3$ state is close to the $3s$ threshold, and this broad resonance causes a large enhancement near the $3s$ threshold. If the energy difference between the $3s$ and $3p$ thresholds was smaller so as to exclude the $n=3$ states, we would anticipate a monotonically increasing average collision strength.

The model calculation represents the dominant contribution (> 50%) to the total collision strength. If we assume that a similar averaged resonant enhancement is applicable for the other contributions, all of which have different energy thresholds, then we obtain the dot-dashed curves of Figs. 1–3. We have further assumed unit branching rates for the resonant-excitation—double-autoionization process, i.e., every $2p^53s^3pnl$ resonant state autoionizes to $2p^53s^2$, which, in turn, autoionizes to $2p^6$. When this additional REDA effect is added to the direct-ionization contribution, the calculated total ionization cross section exhibits a trend which is similar to that found in the experiments.

We note that the energy difference between $3s$ and $3p$ threshold increases linearly as the atomic number Z increases, whereas the positions of the resonances fall farther below the $3p$ threshold as Z^2 for a given principal quantum number n . Thus, as Z increases, the lower n values will get cutoff. For Fe^{15+} , LaGattuta and Hahn⁴ obtained a cutoff at $n=11$ for s states. In addition, as Z increases, the assumption of unit branching ratios breaks down, as pointed out, for example, by Goldberg *et al.*¹⁸ and Cowan and Mann.¹⁹

We conclude that the experiments of Crandall *et al.*¹ on the total ionization cross sections for Na-like Mg^+ , Al^{2+} , and Si^{3+} by electron impact include measurements of the direct-ionization, inner-shell excitation-autoionization, and inner-shell resonant-excitation—double-autoionization physical processes. The direct-ionization and inner-shell ex-

citation (both direct and resonant) processes are probably additive. Other measurements,²⁰ for example, electron-impact ionization of Ti^{3+} , probably exhibit the above three processes.

Differences between distorted-wave theory⁹ and measurements¹ for the direct-ionization contribution to Na-like ions show that a better understanding of the underlying physics is necessary. Further, it is not understood why the simpler plane-wave Born-approximation results¹¹ agree better with the measurements than do those in the distorted-wave approximation. An investigation of potential interference effects between direct-ionization and inner-shell excitation contributions to total ionization cross sections is also necessary. Finally, in order to extrapolate results to more highly charged ions, allowance will have to be made for the increas-

ingly nonunity character of the branching ratio. Additional experiments on electron-impact ionization, particularly interacting beams experiments with more highly charged ions, are eagerly awaited.

ACKNOWLEDGMENTS

Research was supported in part by the U.S. Department of Energy, Office of Basic Energy Sciences. We are grateful for the computing facilities provided by Louisiana State University Systems Network Computer Center. We thank the authors of Refs. 1 and 3 for copies of their results prior to publication, and we thank them for several stimulating discussions. We thank C. H. Greene and A. R. P. Rau for discussions.

¹D. H. Crandall, R. A. Phaneuf, R. A. Falk, D. S. Belic, and G. H. Dunn, *Phys. Rev. A* **25**, 143 (1982).

²D. H. Crandall, *Phys. Scr.* **23**, 153 (1981).

³D. C. Griffin, C. Bottcher, and M. S. Pindzola, *Phys. Rev. A* **25**, 154 (1982).

⁴K. J. LaGattuta and Y. Hahn, *Phys. Rev. A* **24**, 2273 (1981).

⁵A. R. P. Rau (private communication).

⁶E. Clementi and C. Roetti, *At. Data Nucl. Data Tables* **14**, 177 (1974).

⁷A. Hibbert, *Comput. Phys. Commun.* **9**, 141 (1975).

⁸R. J. W. Henry, S. P. Rountree, and E. R. Smith, *Comput. Phys. Commun.* **23**, 233 (1981).

⁹S. M. Younger, *Phys. Rev. A* **24**, 1272 (1981).

¹⁰M. S. Pindzola (private communication).

¹¹E. J. McGuire, *Phys. Rev. A* **26**, 125 (1982).

¹²U. Fano, *Comments At. Mol. Phys.* **1**, 159 (1970).

¹³A. K. Pradhan and M. J. Seaton (private communication).

¹⁴M. J. Seaton, *J. Phys. B* **2**, 5 (1969).

¹⁵K. Bhadra and R. J. W. Henry, *Phys. Rev. A* **26**, 1848 (1982).

¹⁶M. Gailitis, *Zh. Eksp. Teor. Fiz.* **44**, 1974 (1963) [*Sov. Phys.—JETP* **17**, 1328 (1963)].

¹⁷D. L. Moores and H. Nussbaumer, *J. Phys. B* **3**, 161 (1970), predicted large jumps for Mg^+ .

¹⁸L. Goldberg, A. K. Dupree, and J. W. Allen, *Ann. Astrophys.* **28**, 589 (1965).

¹⁹R. D. Cowan and J. B. Mann, *Astrophys. J.* **232**, 940 (1979).

²⁰R. A. Falk, G. H. Dunn, D. C. Griffin, C. Bottcher, D. C. Gregory, D. H. Crandall, and M. S. Pindzola, *Phys. Rev. Lett.* **47**, 494 (1981).